Supplementary Information

Zr-MOF membranes with ultra-fast water-selective permeation towards intensification of esterification reaction

Guozhen Liu[1,†], Zhenggang Wang[1,†], Cailing Chen[2,*], Jiahui Li[1], Guangyuan Zhou[1], Wenqi Ji[1], Gongping Liu[1,*], Wanqin Jin[1]

[1] State Key Laboratory of Materials-Oriented Chemical Engineering, College of Chemical Engineering, Nanjing Tech University, Nanjing 211816, China

[2] King Abdullah University of Science and Technology (KAUST), Physical Sciences and Engineering Division, Advanced Membranes and Porous Materials (AMPM) Center, Thuwal, Saudi Arabia

[†]These authors contribute equally to this work.

*Corresponding authors:

gpliu@njtech.edu.cn (Dr. G. Liu)

cailing.chen@kaust.edu.sa (Dr. C. Chen).

Contents

1. Experimental Details

1.1 Materials

Zirconium oxychloride octahydrate ($ZrOCl_2 \cdot 8H_2O$, 98 %) and terephthalic acid (H_2BDC, $C_8H_6O_4$, purity 98 %) were provided by Sigma-Aldrich. Formic acid (HCOOH, ≥88.0 %) and methanol (CH_3OH, ≥99.5 %) were purchased from Shanghai Lingfeng Chemical Reagent CO., LTD. N, N-Dimethylformamide (DMF, C_3H_7NO, ≥99.5%) and ethyl acetate ($C_4H_8O_2$) were supplied by Sinopharm Chemical Reagent CO., LTD. Nylon substrates were obtained from Beijing Hai Cheng Shi Jie Guo lü Qi Cai Co., LTD. Deionized (DI) water was used in all the experiments.

1.2 Synthesis and Characterizations

1.2.1 Synthesis of UiO-66 membranes

Owing to excellent solvent-resistance properties, nylon substrate was chosen to support polycrystalline UiO-66 membrane, which was fabricated by contra-diffusion method. The Zr solution and BDC solution were prepared separately. In detail, 0.968 g of $ZrOCl_2 \cdot 8H_2O$ powders were dissolved into the mixed solution containing DMF (180 mL) and formic acid (20 mL). In parallel, a BDC solution of 7.46 g of BDC in the same mixed solution was prepared. After stirring for 30 min, the clear solutions were separately added into the left side and right side of U-shaped glass device separated by nylon substrate (Fig. S1), following by hold at 80 ^oC for different time. The resulted MOF membrane was rinsed by DMF for several times and then immersed into anhydrous methanol for 3 days, during which the solvent was replaced by three times per day. Finally, the membrane was activated by vacuum drying at 160 ^oC for overnight.

1.2.2 Characterizations

The morphology of prepare sample was evaluated by Scanning Electron Microscopy (SEM, Hitachi S-4800) and Atomic Force Microscope (AFM, Bruker Dimension Icon). The elements distribution was investigated by Energy Dispersive X-ray spectrometer (EDX). X-ray diffraction (XRD, MiniFlex600) pattern with 5^o-50^o was recorded to measure the crystal structure. The chemical composition was analyzed by Attenuated total reflectance Fourier transform infrared (ATR-FTIR, Thermo Nicolet 8700) spectra. The thermal stability of samples was analyzed using thermogravimetric analysis (TGA, Netzsch Sta 209F1) with a heating rate

of 10 °C/min under N_2 atmosphere. Porosity of nylon substrate was measured by the gravimetric method.[1] The N_2 adsorption isotherms was recorded using Micromeritics ASAP 2020. The samples were prepared as follows: the resulted UiO-66 membranes were immersed into formic acid solution for several hours to dissolve nylon substrate and then the residual powders were collected. After washing by DI water and drying at 100 °C for 12h, the samples were transferred into the BET tube for surface area and pore size analysis. The organic-vapor adsorption isotherms for water and ethyl acetate were measured at 25, 30, and 35 oC using a BELSOR MAX, BEL Japan Inc. Prior to each isotherm measurement, the sample was activated at 150 °C for 12h.

1.2.2.1 Positron annihilation lifetime spectroscopy (PALS)

Besides the BET analysis, the pore window size of UiO-66 membrane was further evaluated by Positron annihilation lifetime spectroscopy (PALS), wherein a radioactive source of ^{22}Na (0.74 MBq) was sealed in 10 μm thick Kapton film. Then the Kapton film was sandwiched in two stacks of UiO-66 membrane samples. A fast–fast coincidence timing system was used to record positron annihilation lifetimes. A time-to-amplitude converter was used to convert lifetimes and to store timing signals in a multi-channel analyzer (Ortec System). During the characterization process, about two million counts were collected. The obtained PALs spectra were analyzed by a finite-term lifetime analysis method using PATFIT program. The mean pore radius R can be related to *ortho*-positronium (o-Ps) (τ) and its intensity (I) according to the following semi-empirical equation:

$$\tau = \frac{1}{2}\left[1 - \left(\frac{R}{R+\Delta R}\right) + \frac{1}{2\pi}\sin\left(\frac{2\pi R}{R+\Delta R}\right)\right]^{-1} \#(1)$$

where R is the pore radius and ΔR is an empirical parameter. Here, ΔR is 1.656 Å

1.3 Performance evaluation

The separation performance of MOF membrane was measured by the home-made pervaporation apparatus. The pressures of permeate side was hold at ~200 Pa. Generally, the flux (J) and separation factor (α) are used to evaluated the separation performance, which could be calculated according to the following equations:

$$J = \frac{M}{A \times t} \# \quad (2)$$

$$\alpha = \frac{Y_i/(1 - Y_i)}{X_i/(1 - X_i)} \#\ (3)$$

where M (g) is the weight of permeate samples, t (h) stands for the operating time and A (m^2) represents the effective membrane area. Xi and Yi stand for the concentration of component i in feed and permeate sides. The concentrations of components were analyzed by gas chromatography (GC).

2. Results and Discussions

Although polymeric substrates have been broadly employed for MOF membranes with low connectivity (e.g., ZIF-8, the connectivity is 4), UiO-66 membrane on polymer support has not been fully demonstrated yet. In this work, continuous UiO-66 membrane was synthesized by that metal sources and ligands source diffused in opposite direction to react at the surface of nylon substrate (Fig. S1), which have two separated ligand and metal source solutions, through isolation by the porous nylon substrate.[2] When the metal and ligand solutions were prepared in the same solvent mixture, controlling the metal and ligand concentrations would allow control over the membrane position (the substrate surface, inside the substrate) based on the diffusion rate difference between metal source and ligand source. Here, the concentration of ligand source for membrane preparation was 0.225 mmol/mL, which is much larger than that of metal source (0.015 mmol/mL), leading to a higher osmotic pressure difference for ligand source. Therefore, the diffusion rate of ligand source is significantly higher than that of metal source. Considering that the metal source is static, while ligand could continuously permeate through porous substrate. When the reactants encounter each other, the initial nucleation preferentially occurred on the substrate surface. With the incessant permeation of ligands, the resulted MOF crystals could grow up gradually, resulting in well inter-grown MOF membranes on the surface of the substrate. [3]

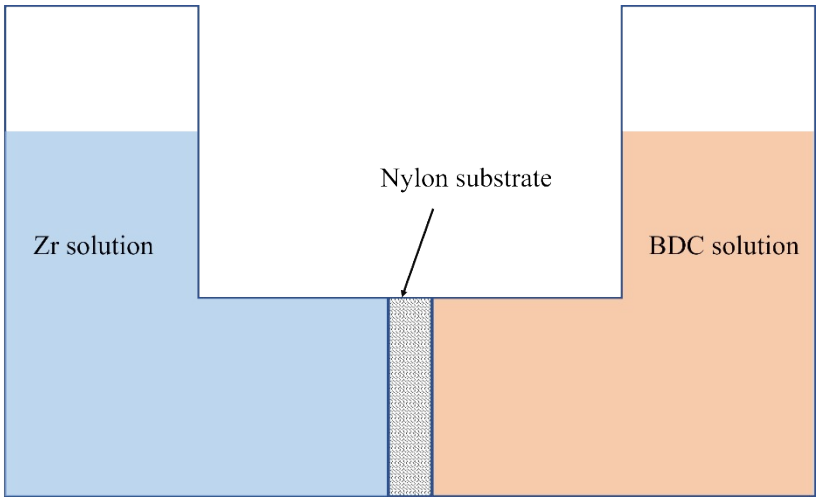

Fig. S1 The schematic image of the set-up for UiO-66 membrane formation

Here, the porous nylon membrane with mean pore size of ~120 nm was selected as the substrate given its merits including excellent solvent-solvent resistance, low transport resistance, and outstanding mechanical strength (Figs. S2-4). It is worth nothing that in the contra diffusion method for MOF membrane preparation, the membrane thickness mainly depends on the metal and ligands concentration. Relatively high reactant concentrations will result in relatively thick layers [3-6].

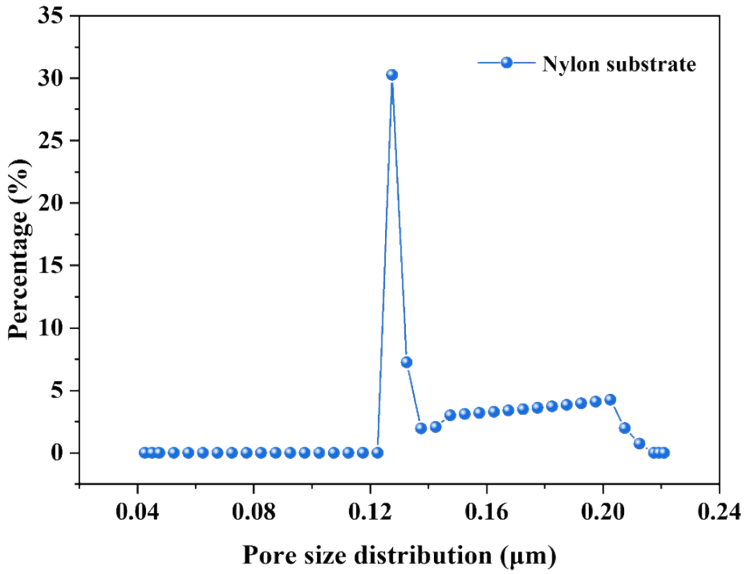

Fig. S2 Pore size distribution of the nylon substrate.

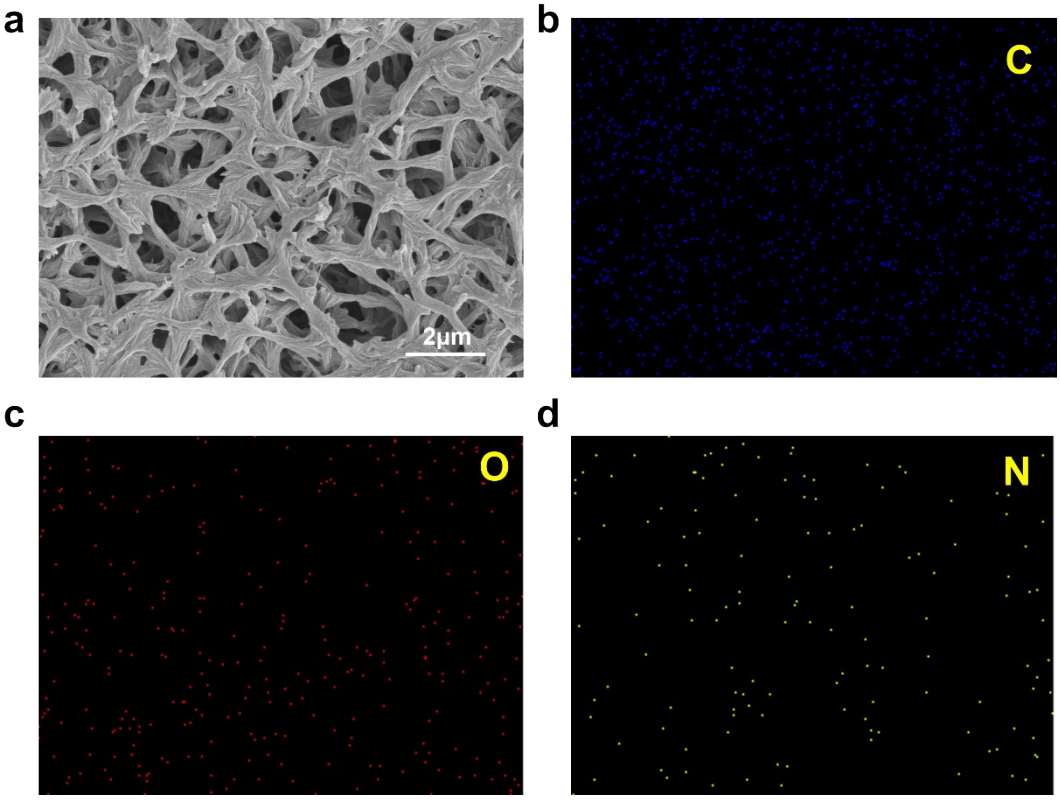

Fig. S3 (a) SEM surface image of nylon substrate. (b)-(d) EDX mapping of C, O, N elements from (a).

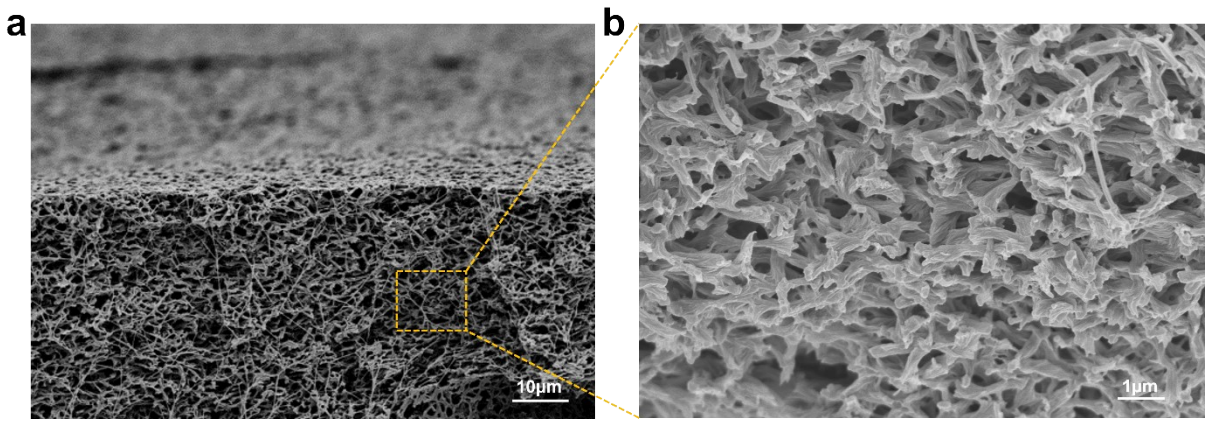

Fig. S4 (a) SEM cross-sectional image of nylon substrate, (b) the enlarged image of area chosen by orange dashed box in (a).

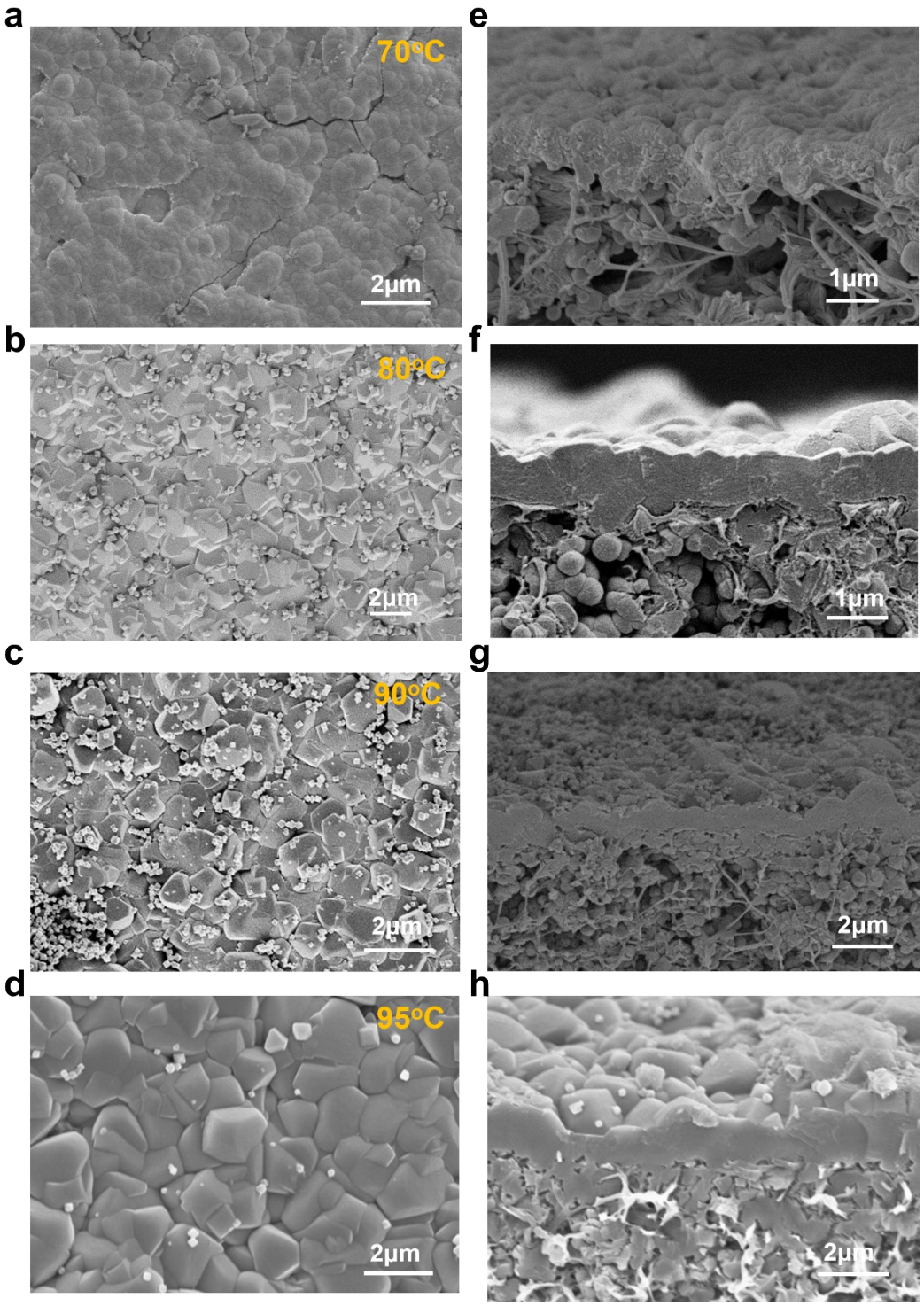

Fig. S5 SEM image of UiO-66 membranes with synthesis temperature of 70-95 °C, the synthesis time is 6 h.

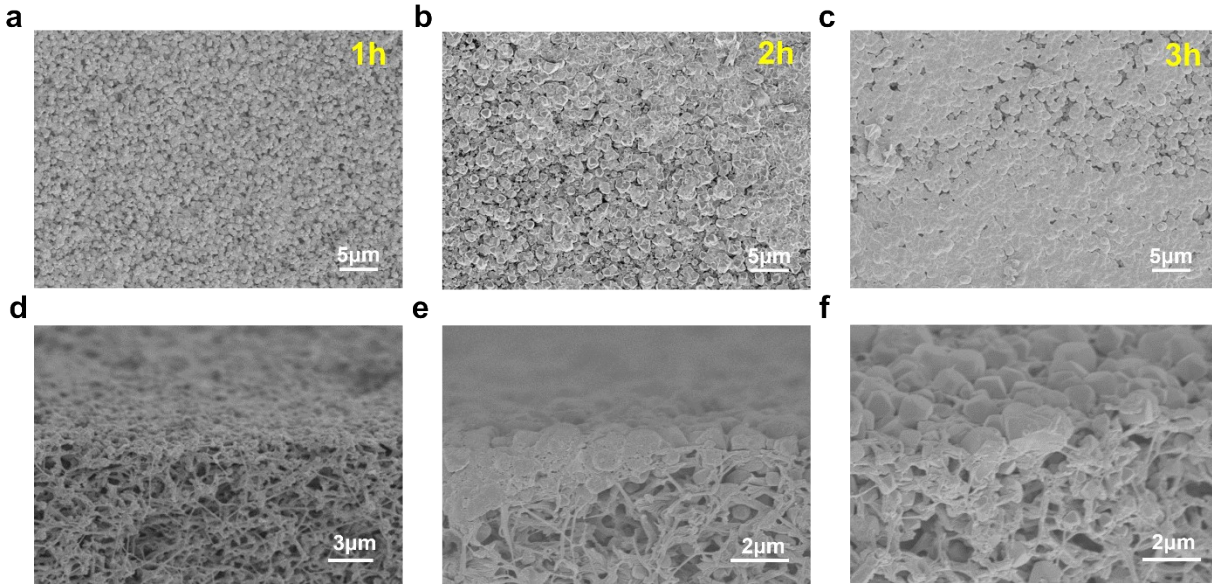

Fig. S6 SEM image of UiO-66 membranes with synthesis time of 1-3h.

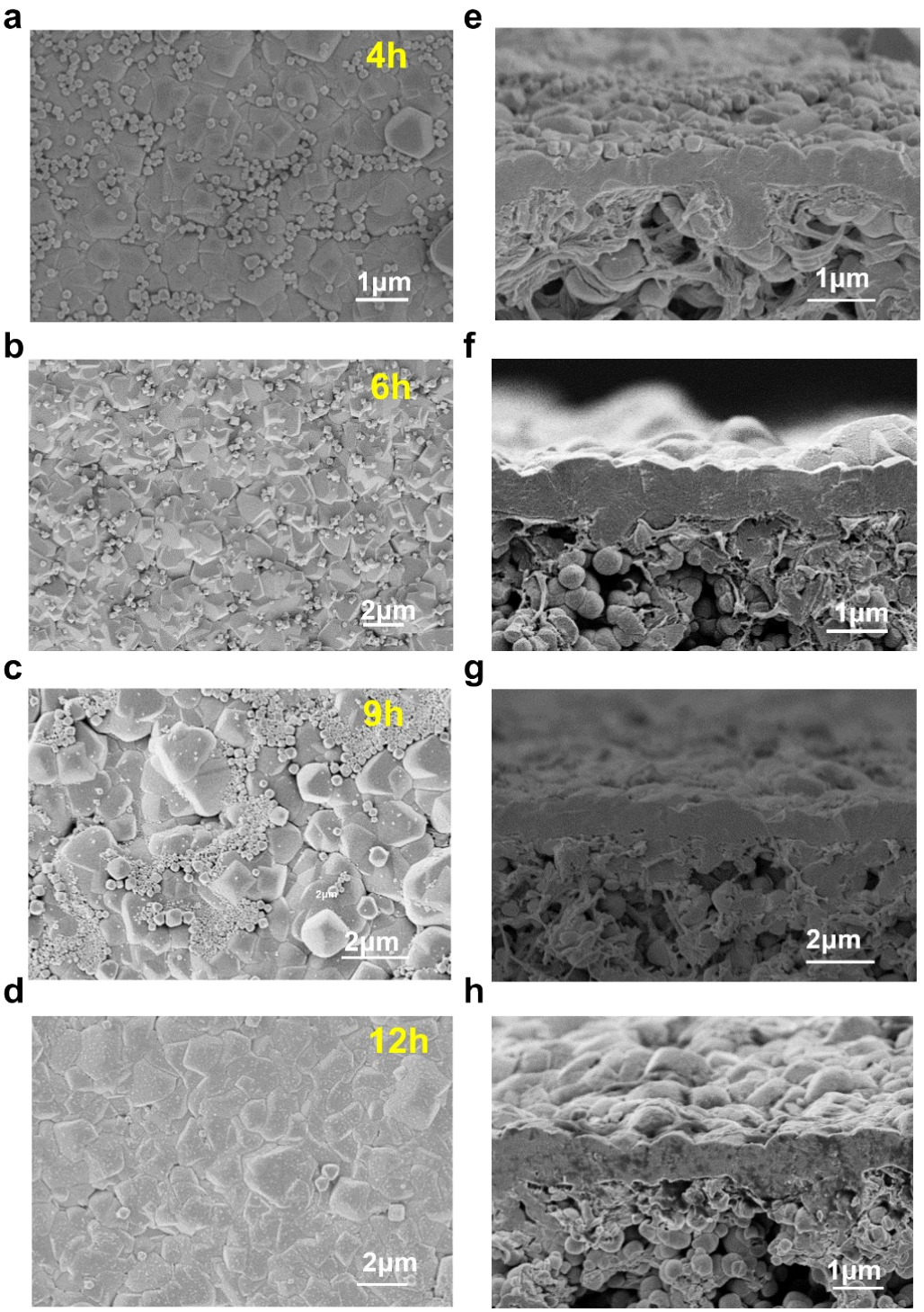

Fig. S7 SEM image of UiO-66 membranes with synthesis time of 4-12h.

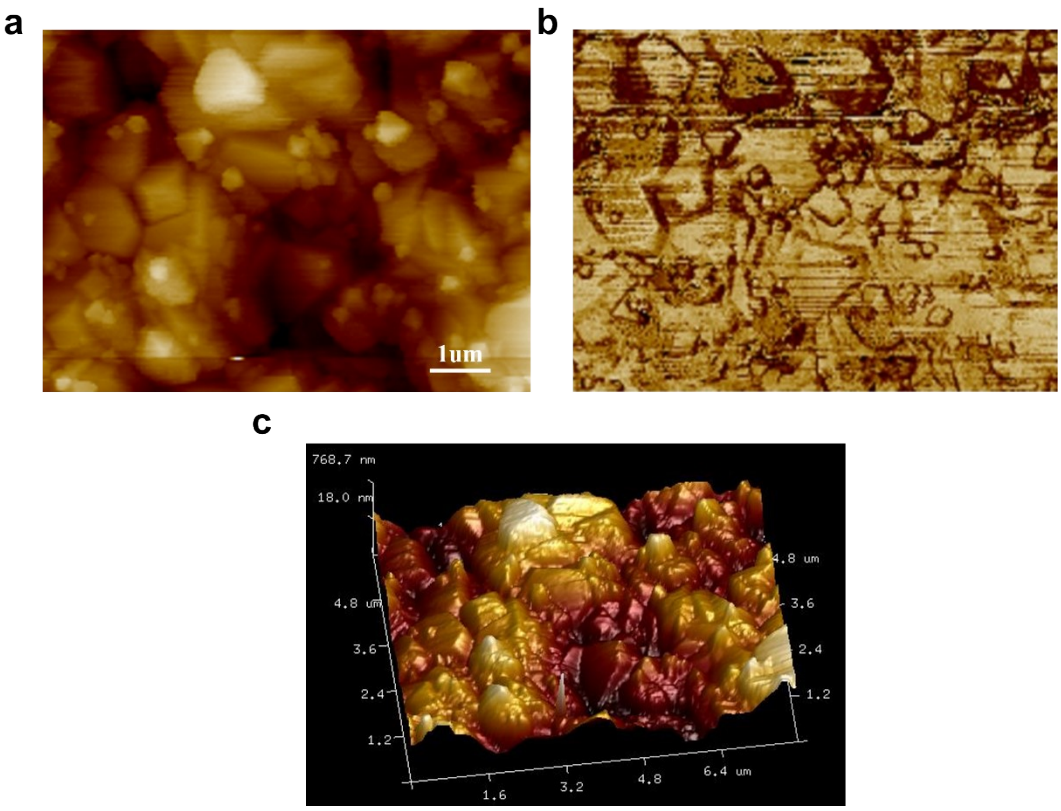

Fig. S8 (a) AFM image of UiO-66 membranes with synthesis time of 4h. The corresponding phase image (b) and 3D image (c).

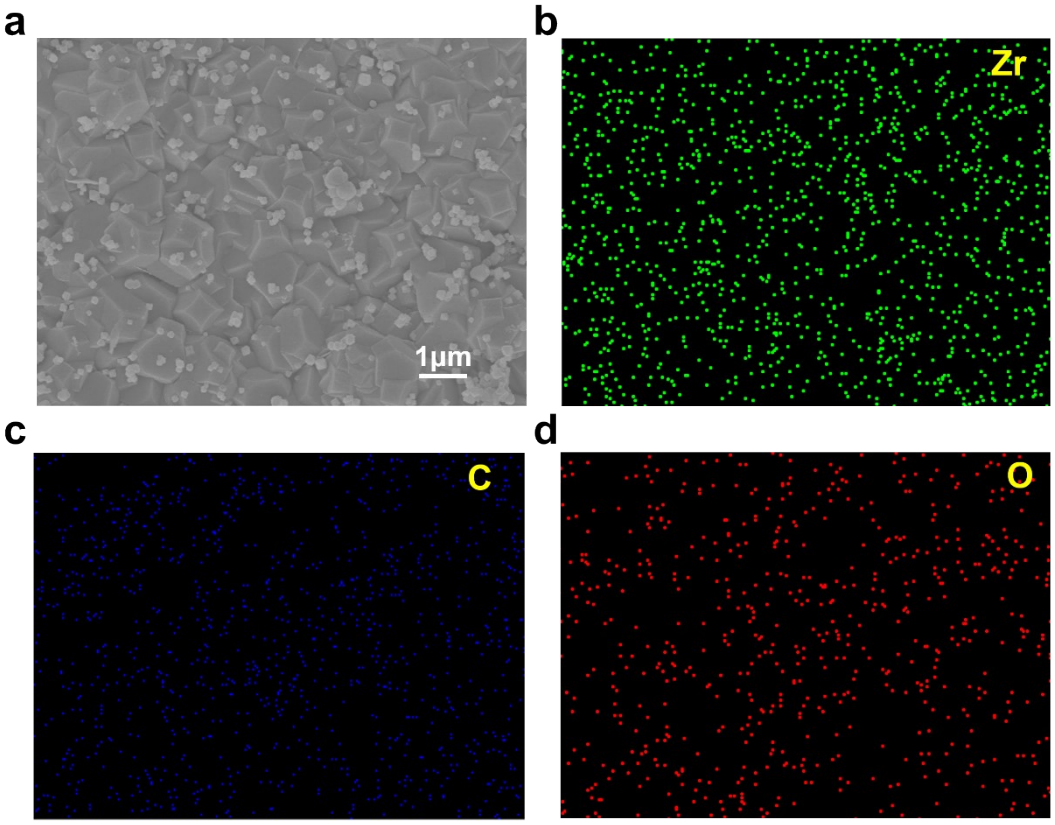

Fig. S9 (a) SEM surface image of UiO-66 membrane with synthesis time of 6h. (b)-(d) EDX mapping of Zr, C, O elements from (a).

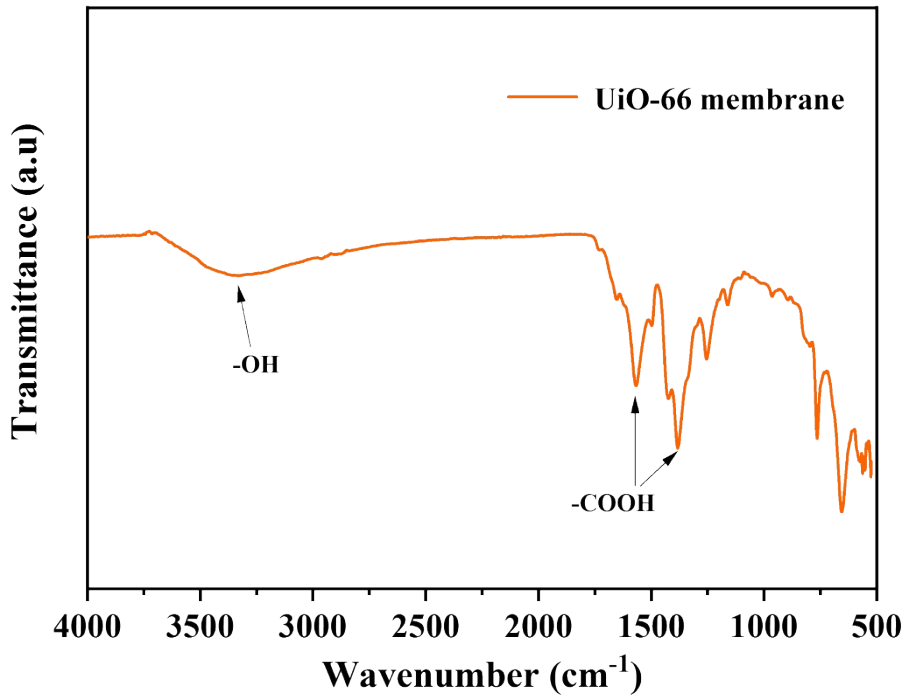

Fig. S10 FTIR spectrum of UiO-66 membrane.

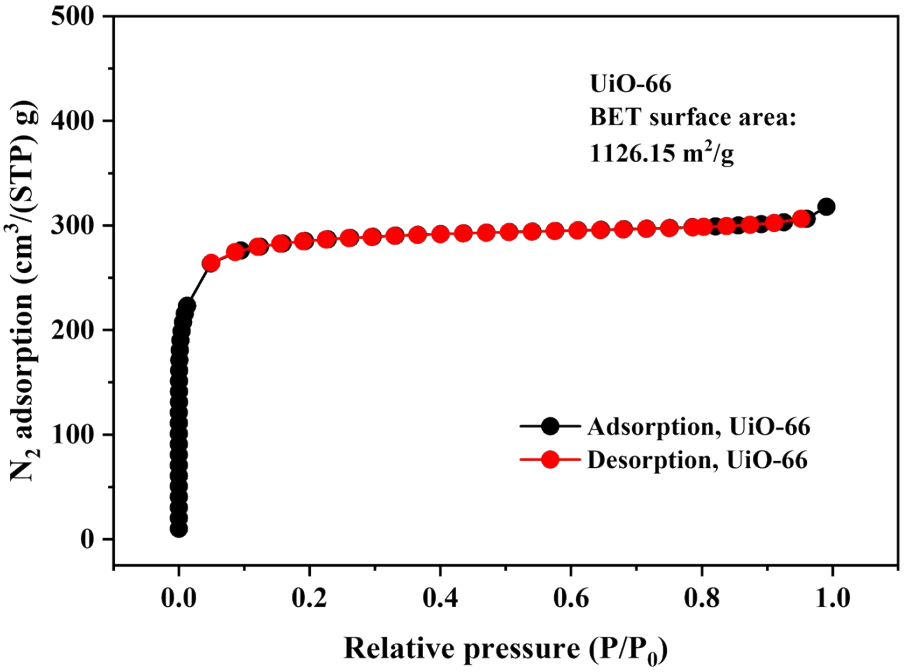

Fig. S11 N_2 adsorption isotherms of UiO-66 membrane.

As show in Fig. S12, the nylon substrate shows a very high flux of ~221 $kg \cdot m^{-2} \cdot h^{-1}$, while the separation factor is only ~1.5, suggesting that there is almost no separation performance for nylon substrate towards ethyl acetate/water mixture.

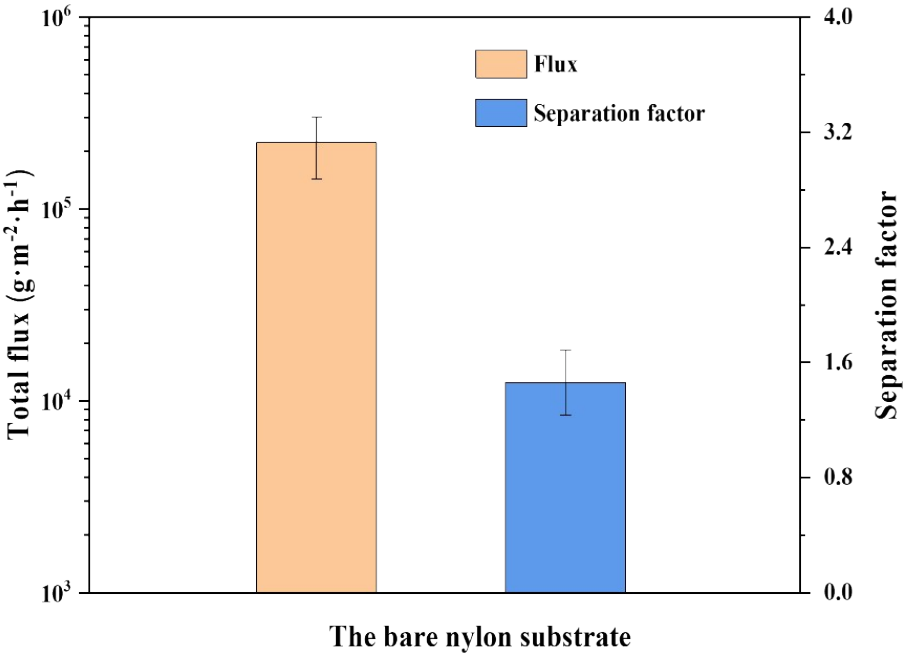

Fig. S12 Separation performance of bare nylon substrate for removing water from ethyl acetate. Feed solution is 98/2 (wt/wt%) ethyl acetate/water mixture and operation temperature is 50 °C.

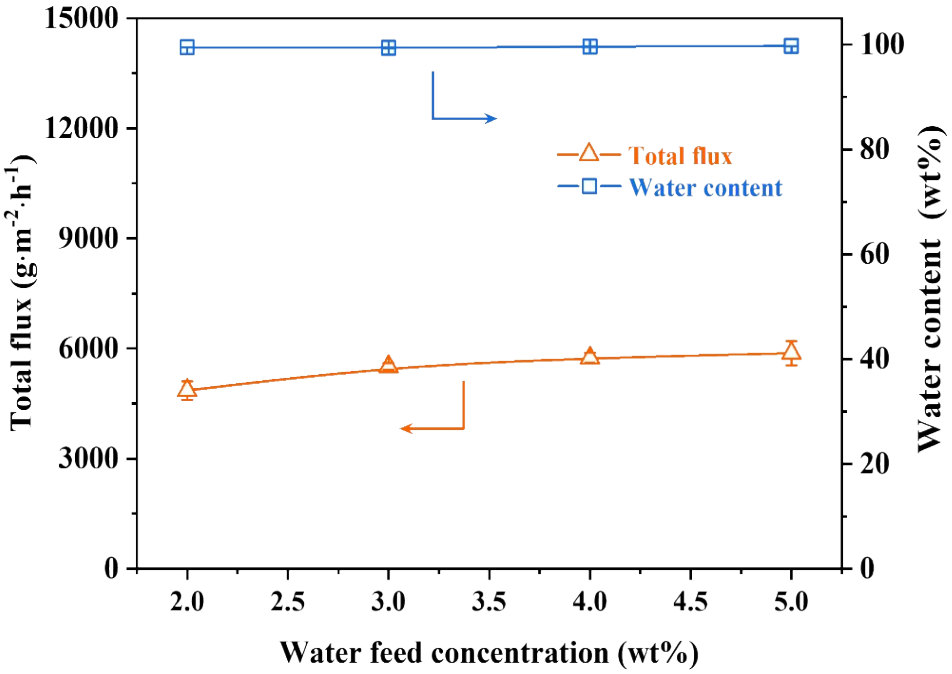

Fig. S13 Effect of water feed concentration on separation performance, the operation temperature is 50 ºC.

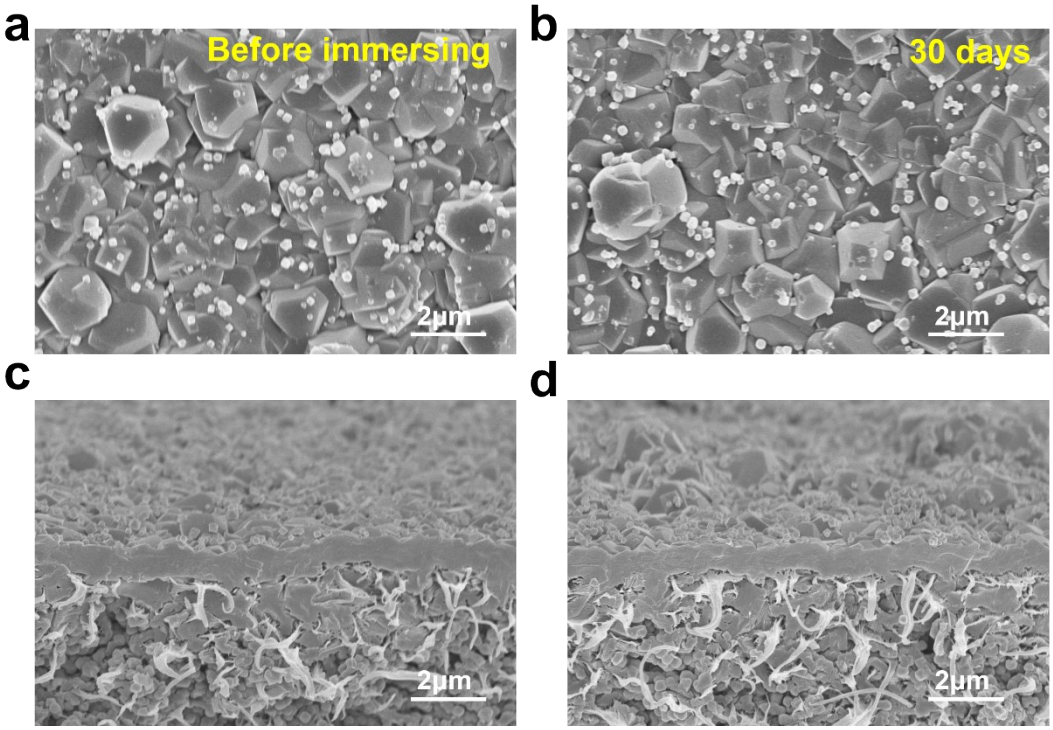

Fig. S14 SEM images of UiO-66 membranes on nylon substrate with synthesis time of 6h before and after immersing into ethyl acetate /water mixture (98/2, wt/wt%) for 30 days.

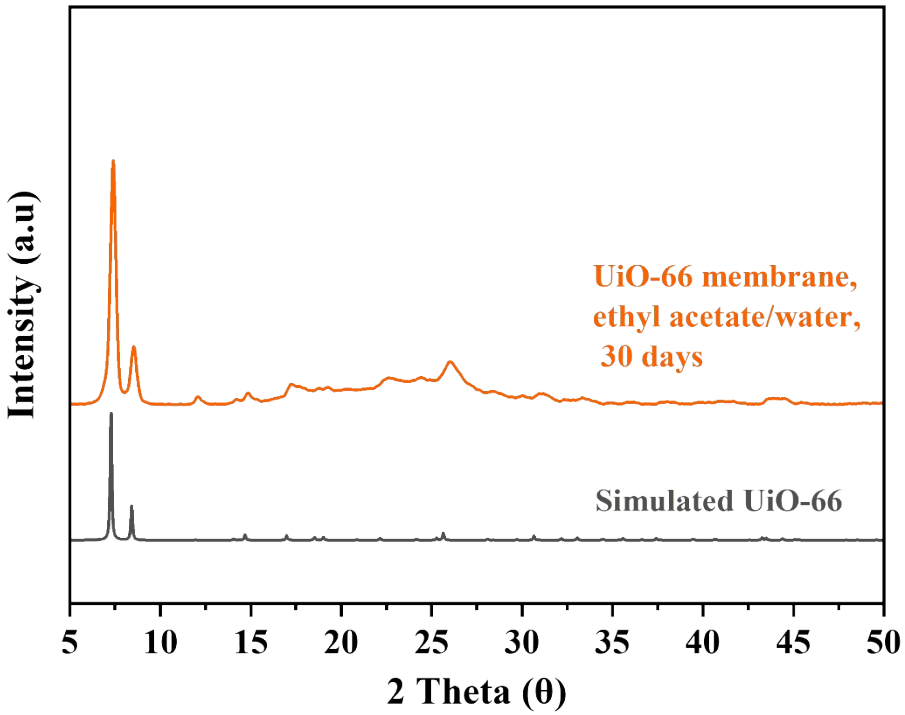

Fig. S15 XRD patterns of UiO-66 membranes on nylon substrate with synthesis time of 6h after immersing into ethyl acetate /water mixture (98/2, wt/wt%) for 30 days.

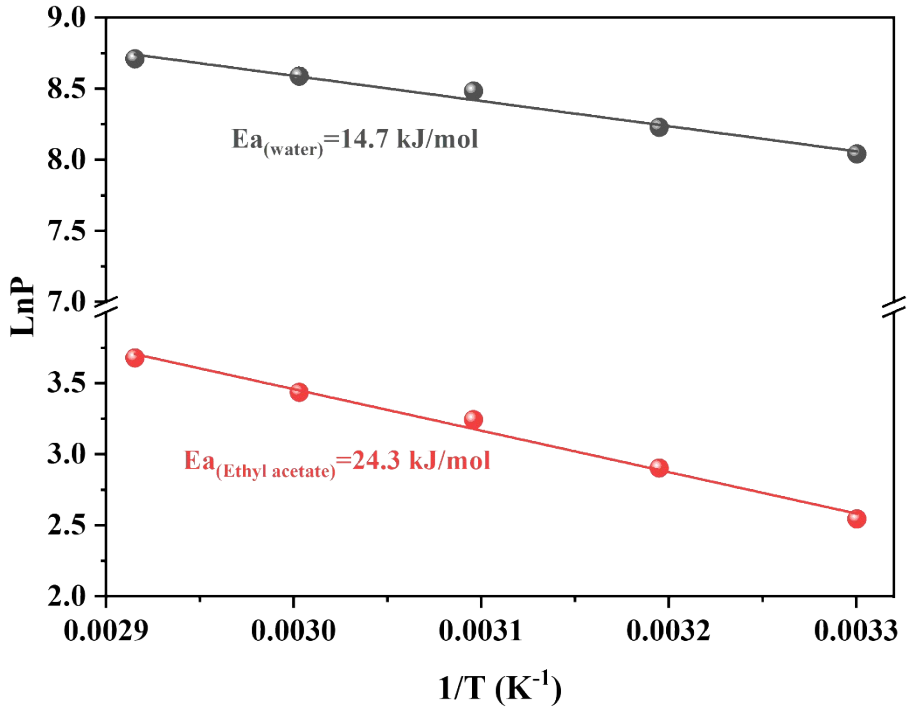

Fig. S16 Arrhenius relationship between water and ethyl acetate flux and feed temperature for UiO-66 membrane.

The adsorption enthalpy of water and ethyl acetate can be calculated based on the following equations[7]:

$$\ln\left(\frac{p}{q}\right) = Aq - \ln K \quad \#\ (4)$$

$$K = K_0 e^{-\Delta H_0/RT} \quad \#(5)$$

where p is the pressure (kPa), q is the water or ethyl acetate adsorbed amounts ($cm^3 \cdot g^{-1}$), A represents a temperature-independent Virial coefficient, and K is the Henry coefficient ($mmol \cdot g^{-1} \cdot bar^{-1}$), the A and K can be obtained according to the adsorbed results of water and ethyl acetate shown in Fig. S17. K_0 is the Henry adsorption constant, ΔH_0 stands for the adsorption enthalpy ($kJ \cdot mol^{-1}$), Generally, adsorption enthalpy is an indication of the interaction between an adsorbent and the adsorbate, which suggests that a higher adsorption enthalpy translates to stronger interactions. R represents the gas constant (8.314 $J \cdot mol^{-1} \cdot K^{-1}$), and T is the absolute temperature (K).

The calculated adsorption enthalpies (ΔH) for water and ethyl acetate were −17.4 kJ mol^{-1} and −27.6 kJ mol^{-1}, respectively.

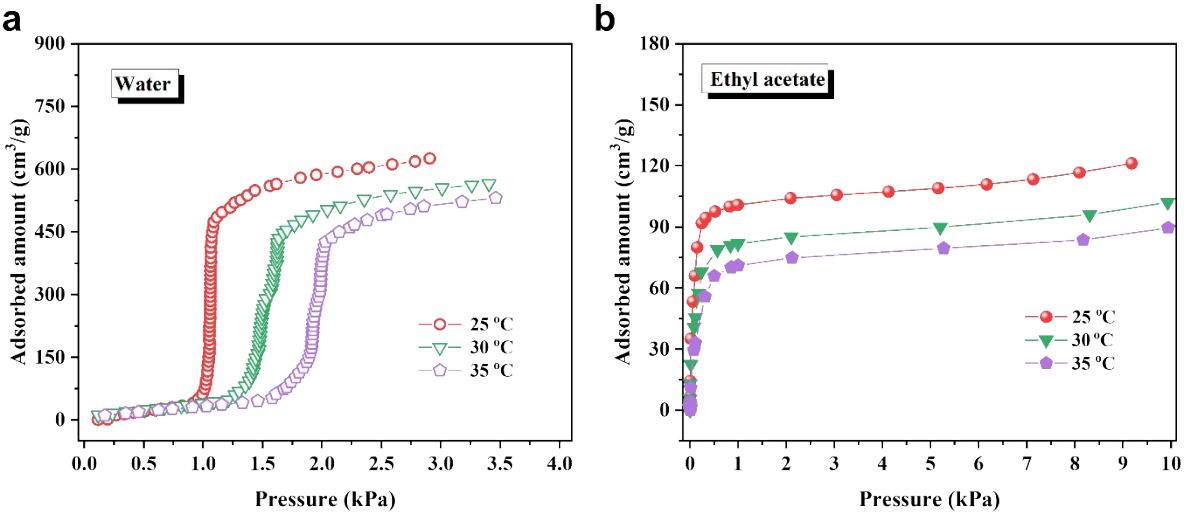

Fig. S17 Isothermal adsorption of UiO-66 towards (a) water and (b) Ethyl acetate at 25, 30 and 35 °C.

It can be expected that UiO-66 membrane with excellent chemical stability and solvent dehydration performance could be employed in practical coupling system of esterification and pervaporation solvent dehydration, wherein the byproduct water can be in-situ removed by pervaporation membrane to enhance the conversion rate of esterification reaction.

Tab. S1 Performance comparison of UiO-66 membrane on ethyl acetate /water separation with state-of-the-arts membranes

Membrane	T(K)	Feed water concentration (wt%)	Total flux ($g \cdot m^{-2} \cdot h^{-1}$)	Separation factor	Ref.
Perfluorosulfonic acid-TEOS	313	2.0	205	496	[8]
PBI/PEI	313	2.0	820	2478	[9]
CS	313	2.0	336	6270	[10]
PVA	313	2.0	35	7270	[11]
PVA	323	2.0	22	5000	[12]
UiO-66	323	2.0	3233	6951	[13]
MXene	323	2.0	1471	4898	[14]
VA-PFSA-TEOS-GPTMS/PAN	313	2.0	260	6673	[15]
ZSM-5/PEBA/PES	323	5.0	1895	108.52	[16]
PVA/CS	323	2.0	200	>10000	[17]
MIL-53	333	7.0	452	1317	[18]
NaA zeolite	323	2.0	150	>10000	[19]
NaY zeolite	323	2.0	3700	5800	[20]
MCM-48	323	5.0	5780	123	[21]
BTESE	333	2.0	840	>10000	[22]
UiO-66	343	2.0	6100	7500	This work

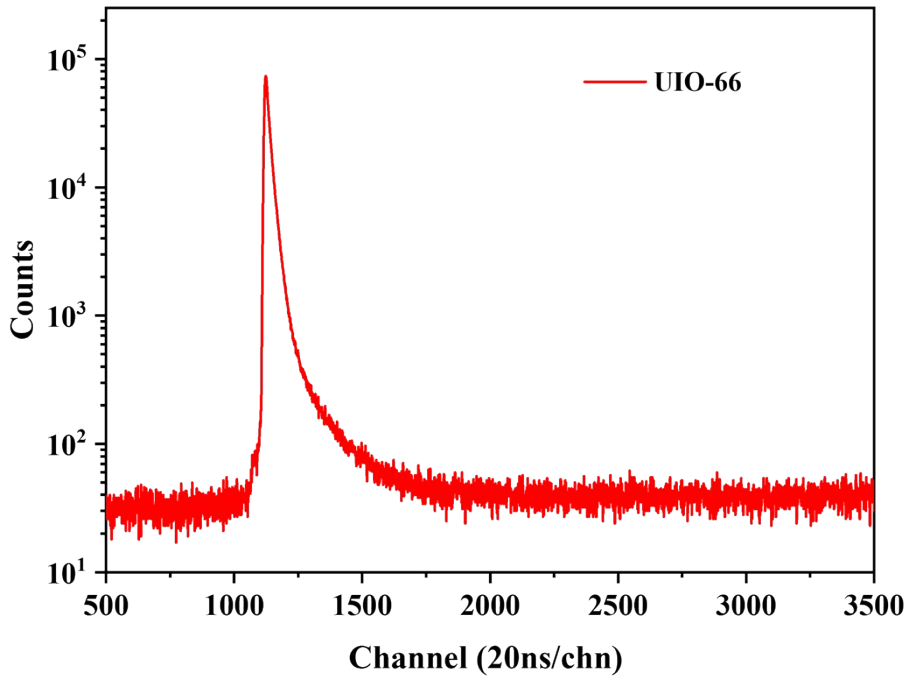

Fig. S18 PALS spectrum of UiO-66 membrane.

3. References

1. X. Zhu, S. S. Feng, S. F. Zhao, F. Zhang, C. Xu, M. Hu, Z. X. Zhong and W. H. Xing, *J. Membr. Sci.*, 2020, **594**, 117473.
2. W. B. Li, *Prog. Mater. Sci.*, 2019, **100**, 21-63.
3. A. J. Brown, N. A. Brunelli, K. Eum, F. Rashidi, J. R. Johnson, W. J. Koros, C. W. Jones and S. Nair, *Science*, 2014, **345**, 72-75.
4. E. Barankova, X. Tan, L. F. Villalobos, E. Litwiller and K.-V. Peinemann, *Angew. Chem. Int. Edit.*, 2017, **56**, 2965-2968.
5. J. F. Yao, D. H. Dong, D. Li, L. He, G. S. Xu and H. T. Wang, *Chemical Communications*, 2011, **47**, 2559-2561.
6. M. He, J. F. Yao, L. X. Li, Z. X. Zhong, F. Y. Chen and H. T. Wang, *Microporous Mesoporous Mat.*, 2013, **179**, 10-16.
7. G. Y. Dong, H. Nagasawa, L. Yu, Q. Wang, K. Yamamoto, J. Ohshita, M. Kanezashi and T. Tsuru, *J. Membr. Sci.*, 2020, **610**, 118284.
8. H.-K. Yuan, Z.-L. Xu, J.-H. Shi and X.-H. Ma, *J. Appl. Polym. Sci.*, 2008, **109**, 4025-4035.
9. Y. Wang, *Ind. Eng. Chem. Res.*, 2015, **54**, 3082-3089.
10. X. H. Ma, Z. L. Xu, C. Q. Ji, Y. M. Wei and H. Yang, *J. Appl. Polym. Sci.*, 2011, **120**, 1017-1024.
11. H. K. Yuan, J. Ren, X. H. Ma and Z. L. Xu, *Desalination*, 2011, **280**, 252-258.
12. Y. Salt, A. Hasanoglu, I. Salt, S. Keleser, S. Ozkan and S. Dincer, *Vacuum*, 2005, **79**, 215-220.
13. Y. P. Ying, D. H. Liu, W. X. Zhang, J. Ma, H. L. Huang, Q. Y. Yang and C. L. Zhong, *ACS Appl. Mater. Interfaces*, 2017, **9**, 1710-1718.
14. Z. Xu, G. Z. Liu, H. Ye, W. Q. Jin and Z. F. Cui, *J. Membr. Sci.*, 2018, **563**, 625-632.
15. H. Yuan, C. Wang, X. Liu and J. Lu, *Polymer Bulletin*, 2021, **78**, 335-358.
16. M. Vatani, A. Raisi and G. Pazuki, *Microporous Mesoporous Mat.*, 2018, **263**, 257-267.
17. Y. X. Zhu, S. S. Xia, G. P. Liu and W. Q. Jin, *J. Membr. Sci.*, 2010, **349**, 341-348.
18. Y. Hu, X. Dong, J. Nan, W. Jin, X. Ren, N. Xu and Y. M. Lee, *Chemical Communications*, 2011, **47**, 737-739.

19. M. M. Shahrestani, A. Moheb and M. Ghiaci, *Vacuum*, 2013, **92**, 70-76.
20. H. Ahn and L. Y. Taek, *Korean Chem. Eng. Res.*, 2005, **43**, 366-370.
21. S. F. Wu, J. Q. Wang, G. L. Liu, Y. Yang and J. M. Lu, *J. Membr. Sci.*, 2012, **390**, 175-181.
22. W. Raza, J. H. Yang, J. X. Wang, H. Saulat, L. Wang, J. M. Lu and Y. Zhang, *J. Appl. Polym. Sci.*, 2021, **138**, e50942.